Supplementary Material (ESI) for Dalton Transactions

Tripodal Imidazole Frameworks: Reversible Vapour Sorption Both With and Without Significant Structural Changes†

Charlotte E. Willans,[a] Sara French,[a] Leonard J. Barbour,[b] Jan-André Gertenbach,[b] Peter C. Junk,[c] Gareth O. Lloyd[a] Robert J. Dyer[a] and Jonathan W. Steed[a*]

Supplementary information

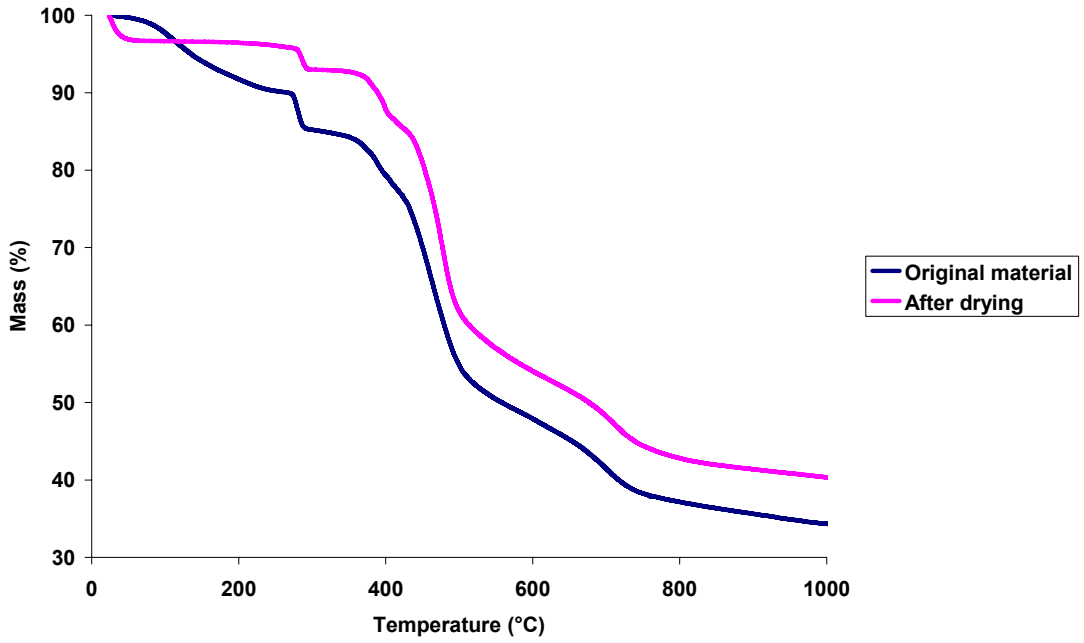

Figure S1: TGA curves for **TIF-1** as synthesised and after heating at 200°C.

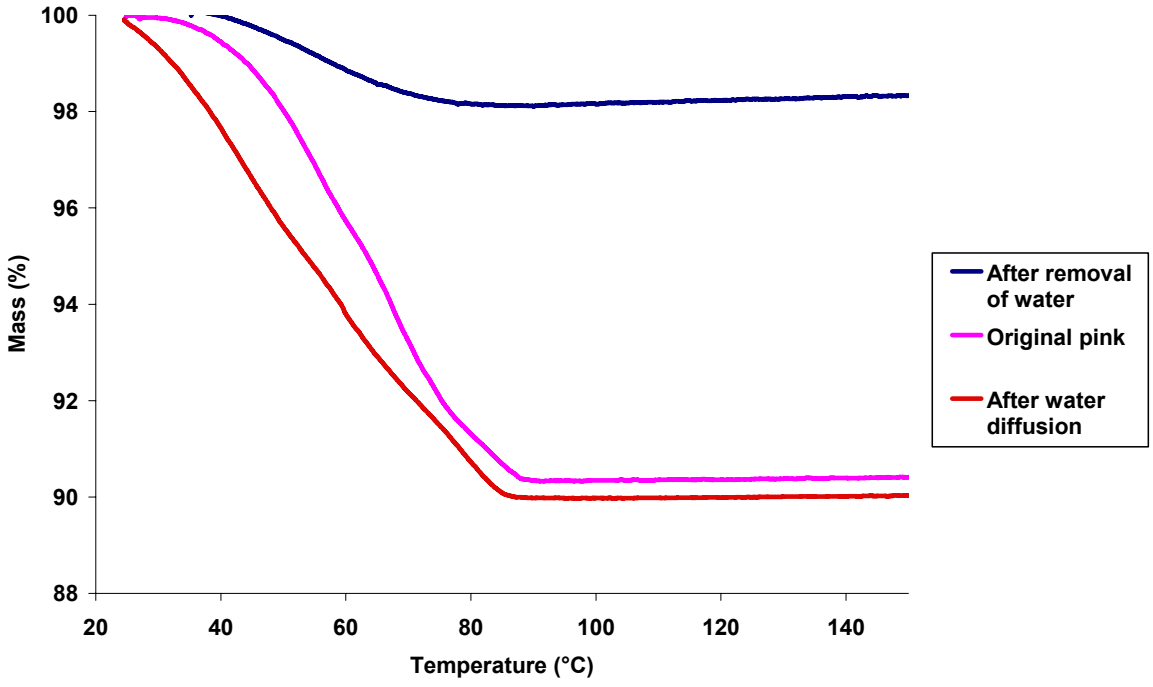

Figure S2: TGA curves for **TIF-2**.

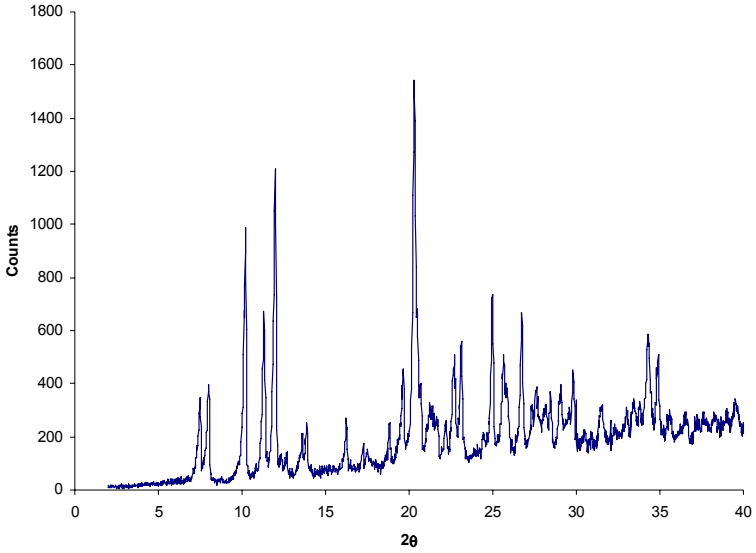

(a)

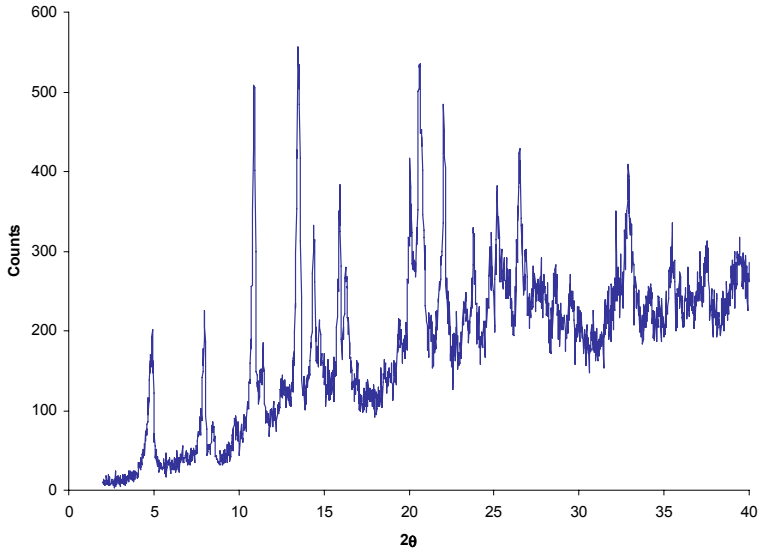

(b)

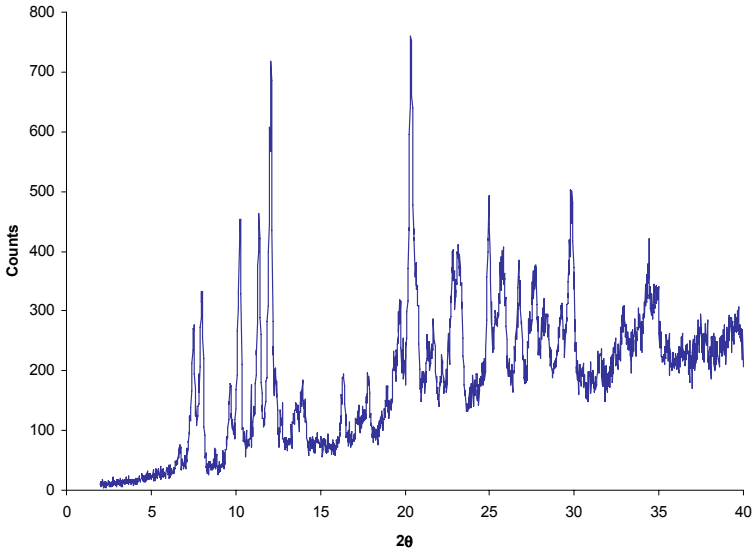

(c)

Figure S3: XRPD Data for **TIF-2** (a) as synthesized (pink) (b) after drying (blue) (c) after exposure of dried material to water (pink)

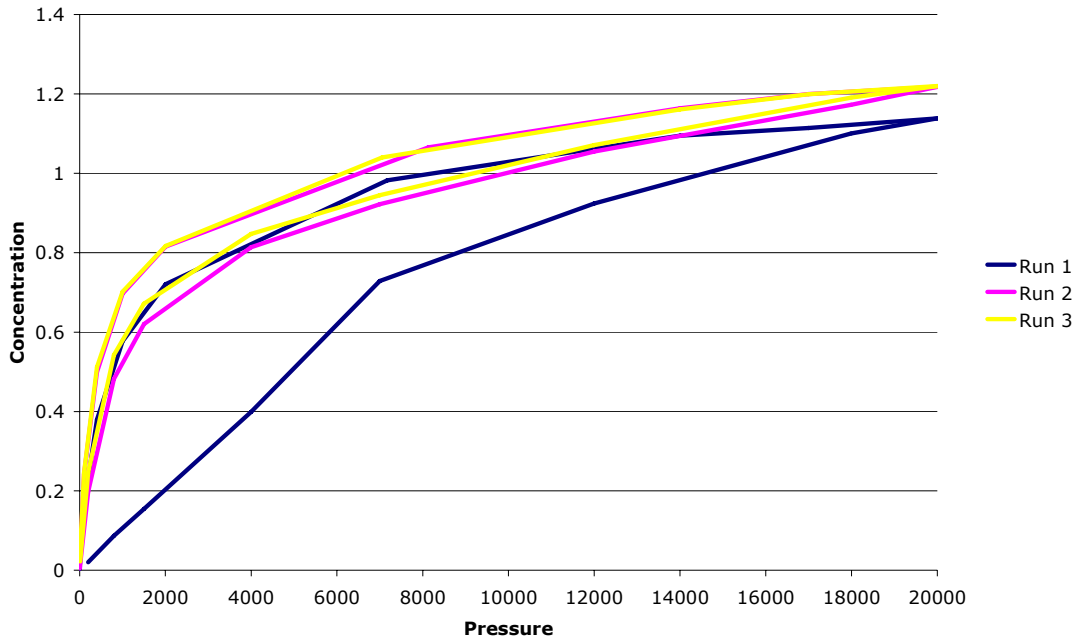

Figure S4: Multiple cycles of CO_2 sorption and desorption of **TIF-2′** at 22 °C.

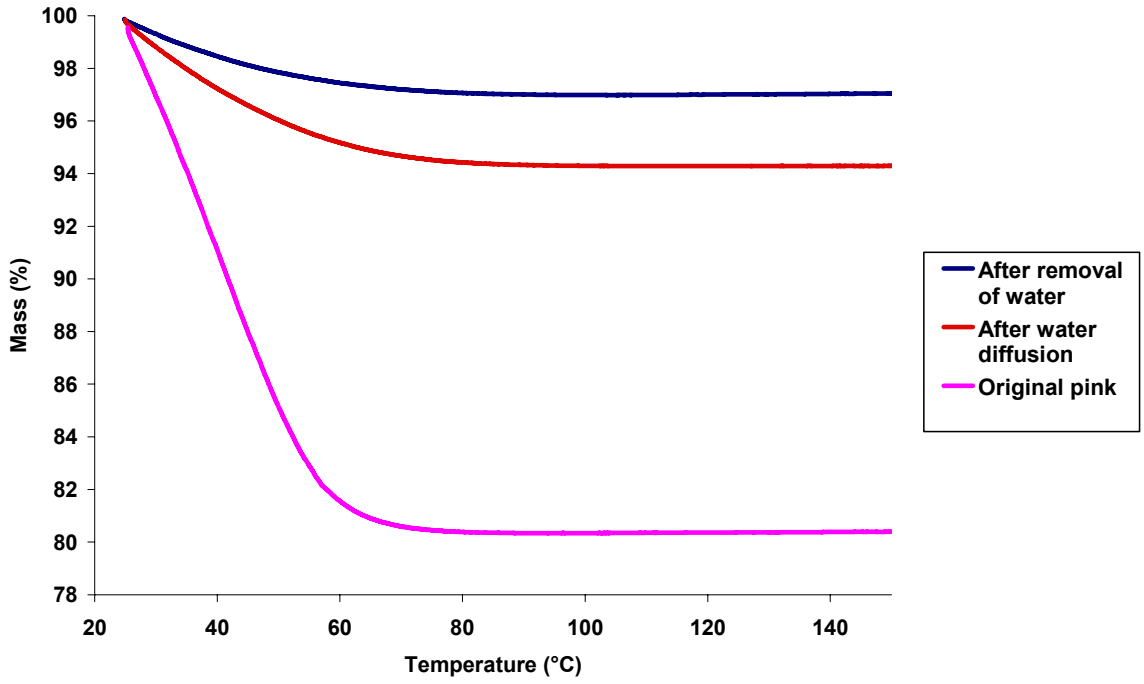

Figure S5: TGA data for **TIF-3**

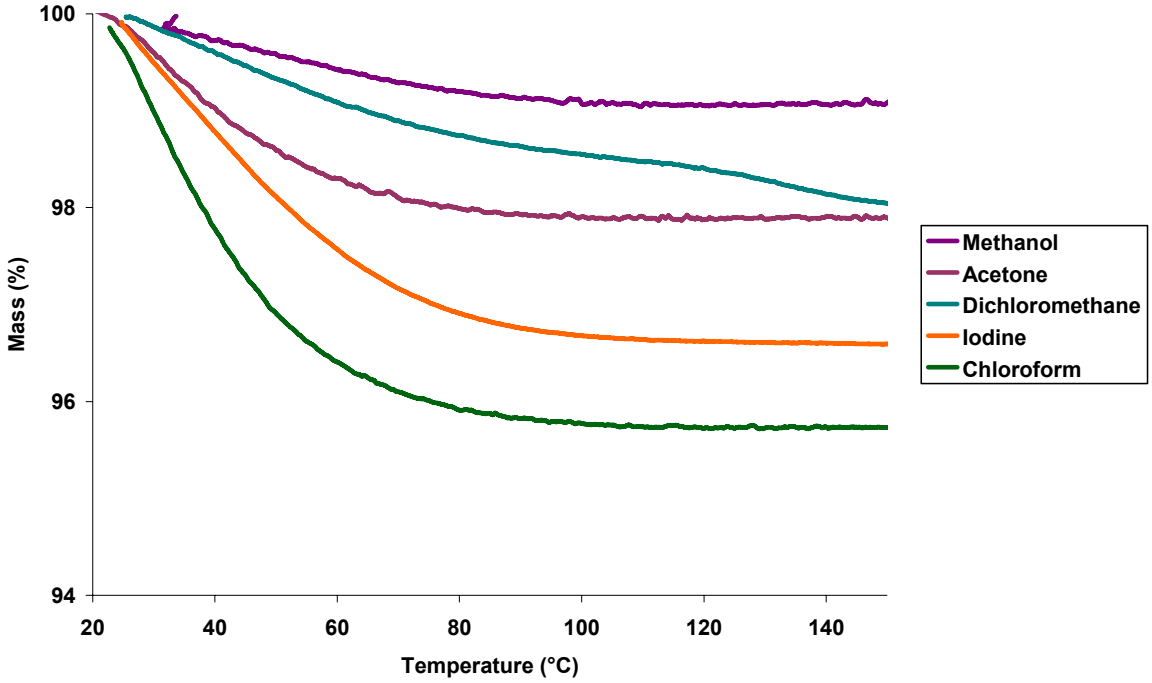

Figure S6: TGA curves for **TIF-3** after exposure to different vapours.

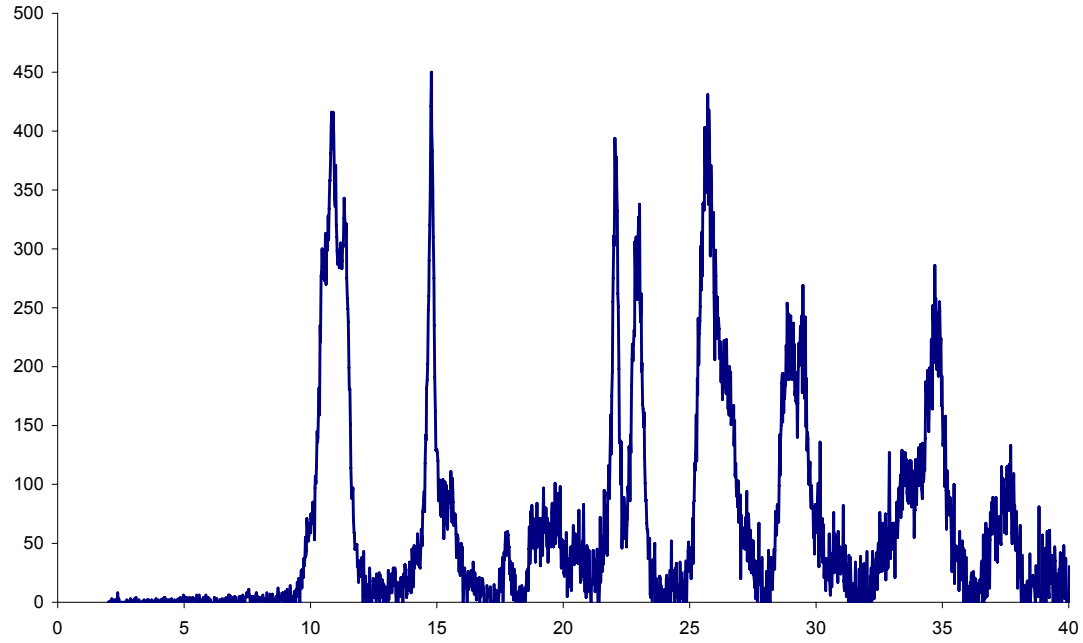

Figure S7: X-ray diffraction powder pattern of dehydrated **TIF-3** after water vapour diffusion.

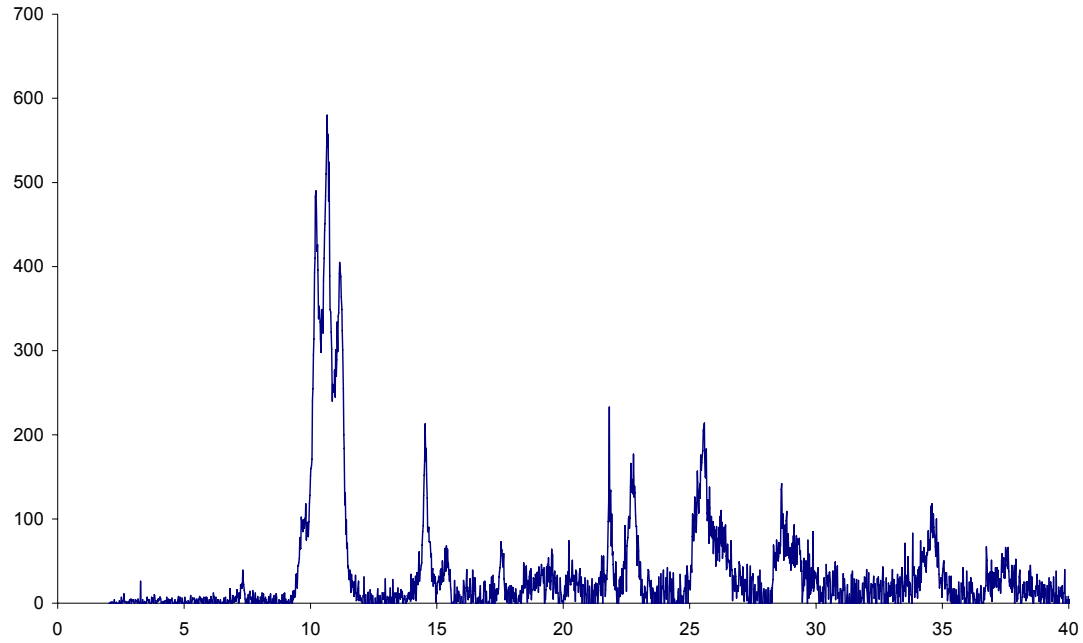

Figure S8: X-ray diffraction powder pattern of dehydrated **TIF-3** after D_2O vapour diffusion**.**

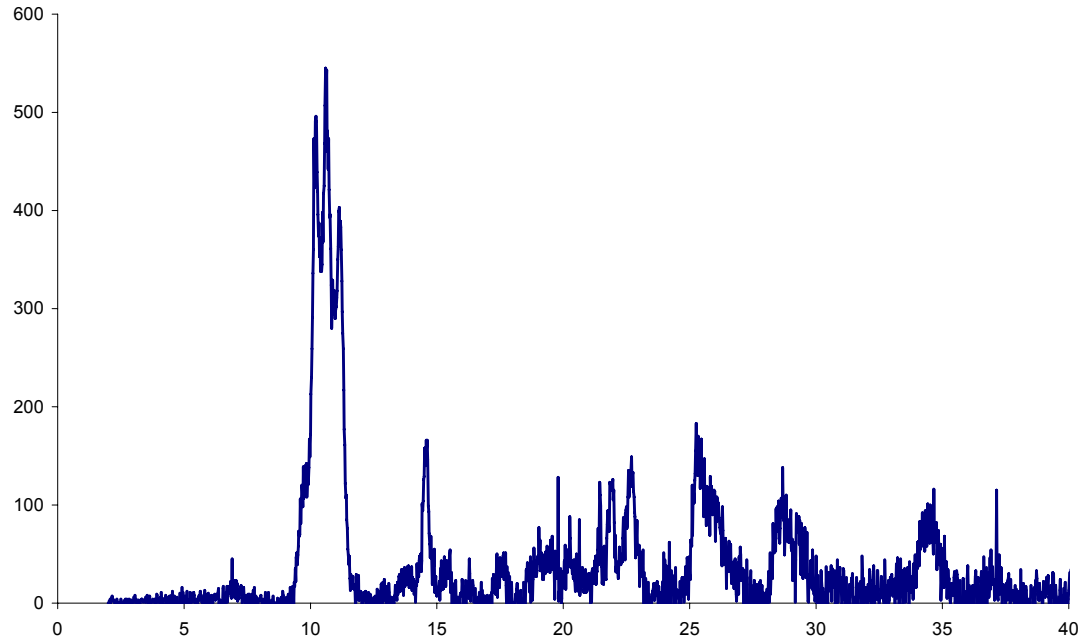

Figure S9: X-ray diffraction powder pattern of dehydrated **TIF-3** after MeOH vapour diffusion**.**

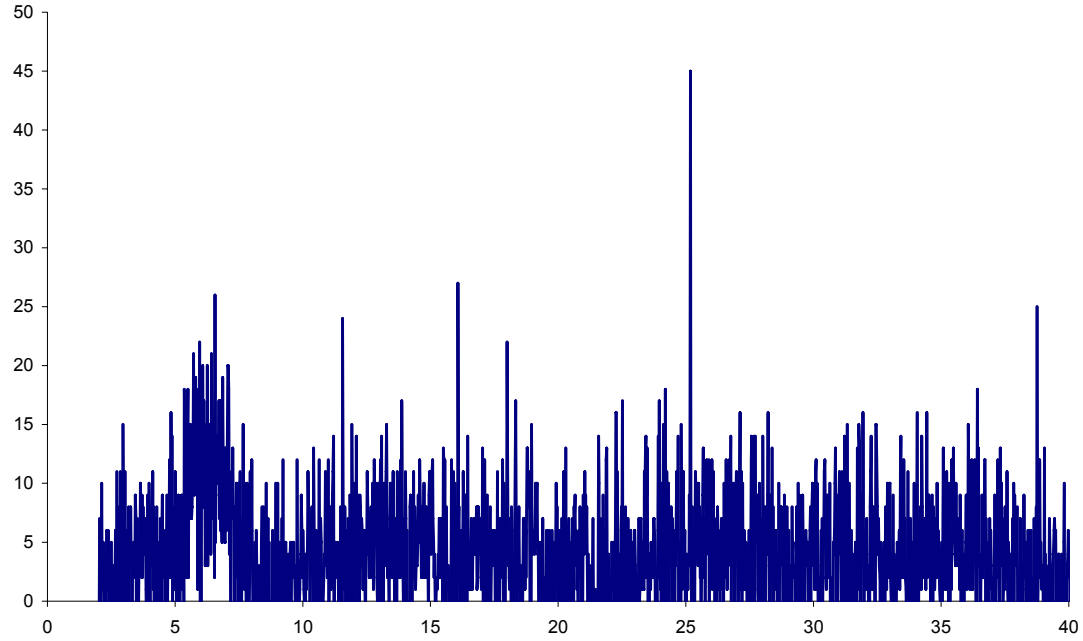

Figure S10: X-ray diffraction powder pattern of dehydrated **TIF-3** after DCM vapour diffusion**.**

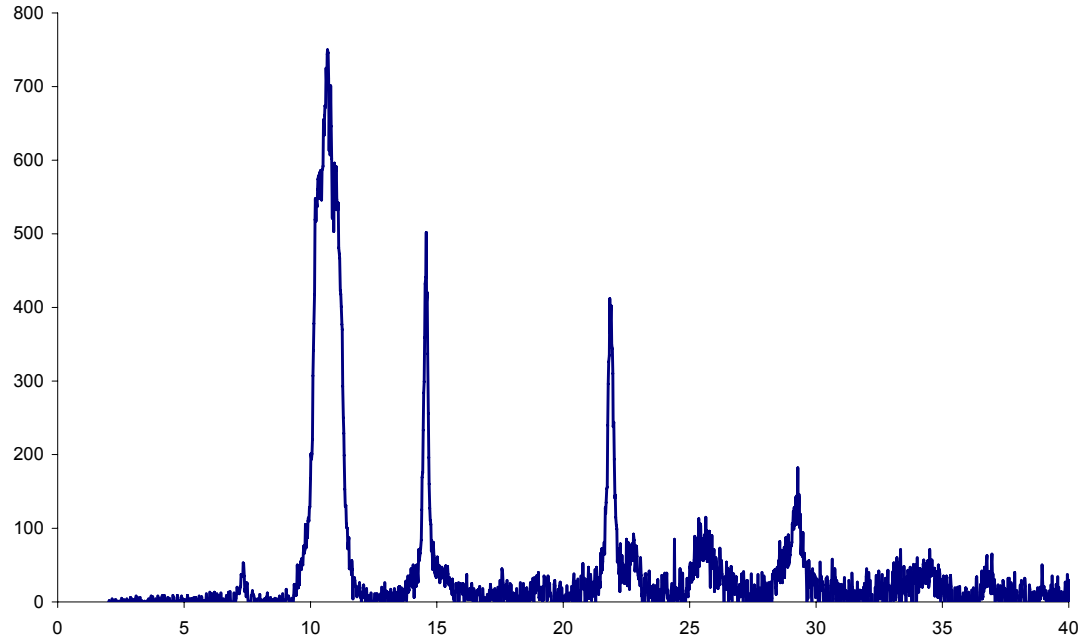

Figure S11: X-ray diffraction powder pattern of dehydrated **TIF-3** after Iodine vapour diffusion.

(a) (b) (c) (d)

Figure S12: solid-state mechanochemical reaction of ligand **1** with copper(II) chloride (a) starting material $CuCl_2 \cdot 2H_2O$, (b) product from grinding $CuCl_2 \cdot 2H_2O$ with **1**, (c) sample in 'b' after drying in an oven at 80 ^oC, (d) material formed from sample shown in 'c' by slow diffusion of water vapour.

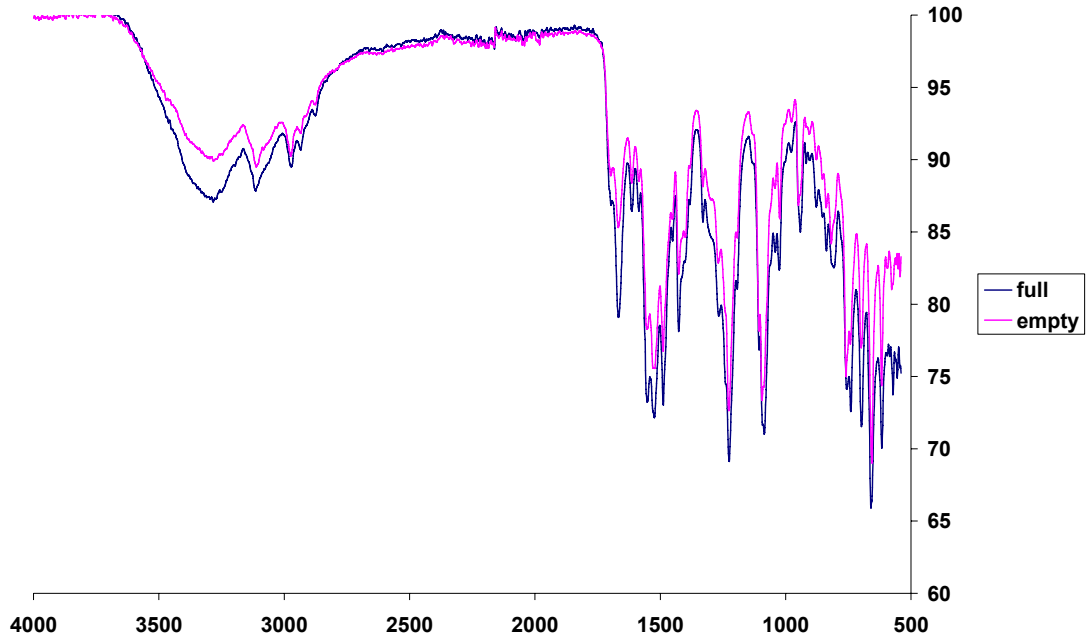

Figure S13: IR spectra of TIF 1.

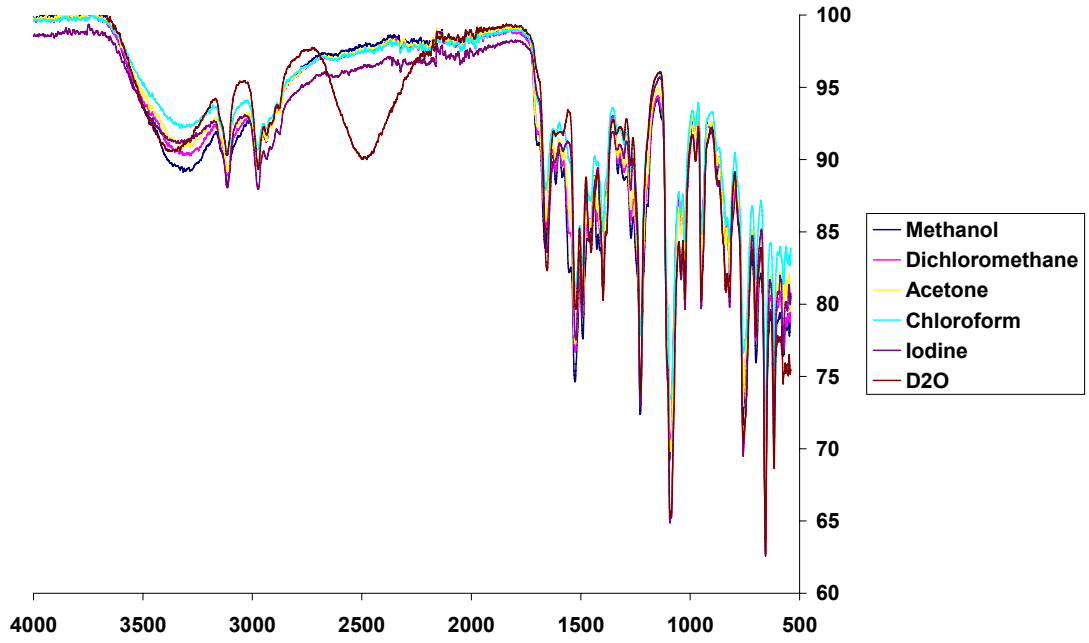

Figure S14: IR spectra of TIF 1 following vapour diffusion.

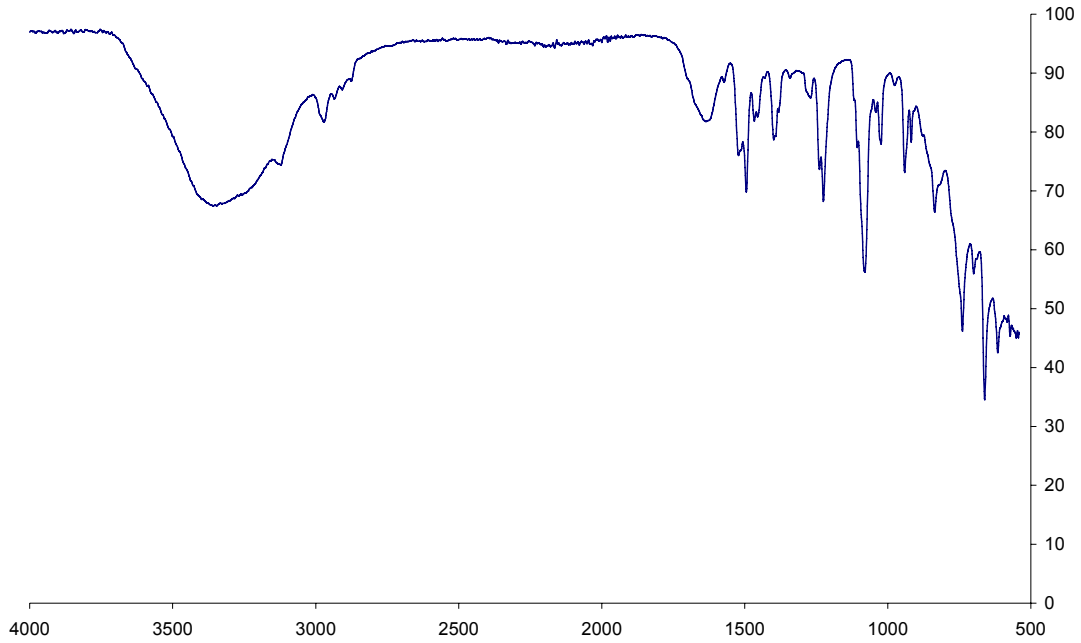

Figure S15: IR spectrum of TIF 2.

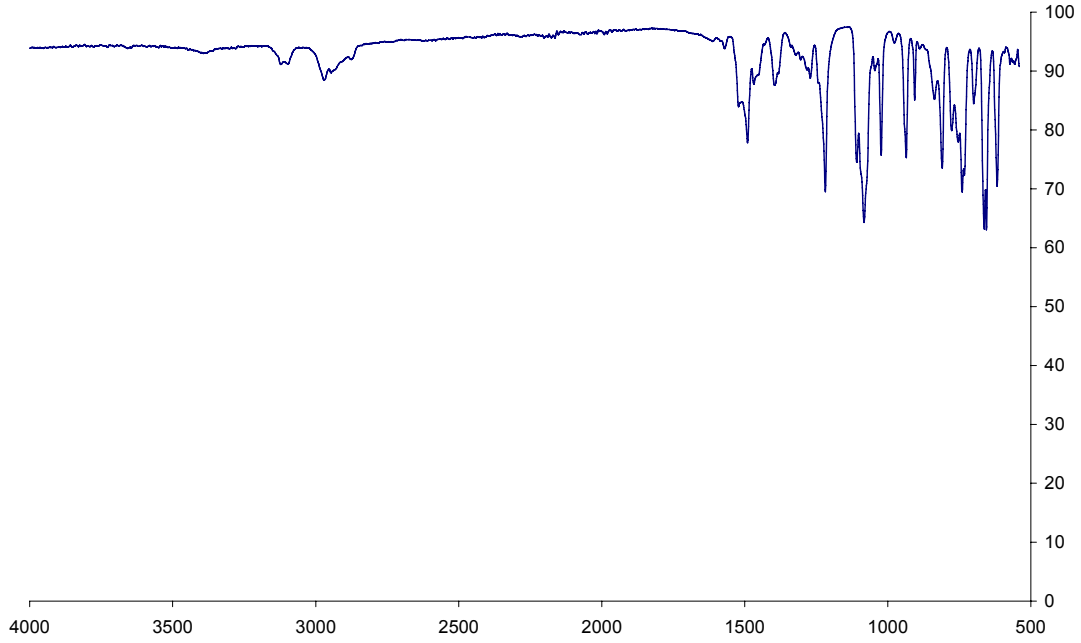

Figure S16: IR spectrum of TIF 2 after heating at 80 °C under vacuum.

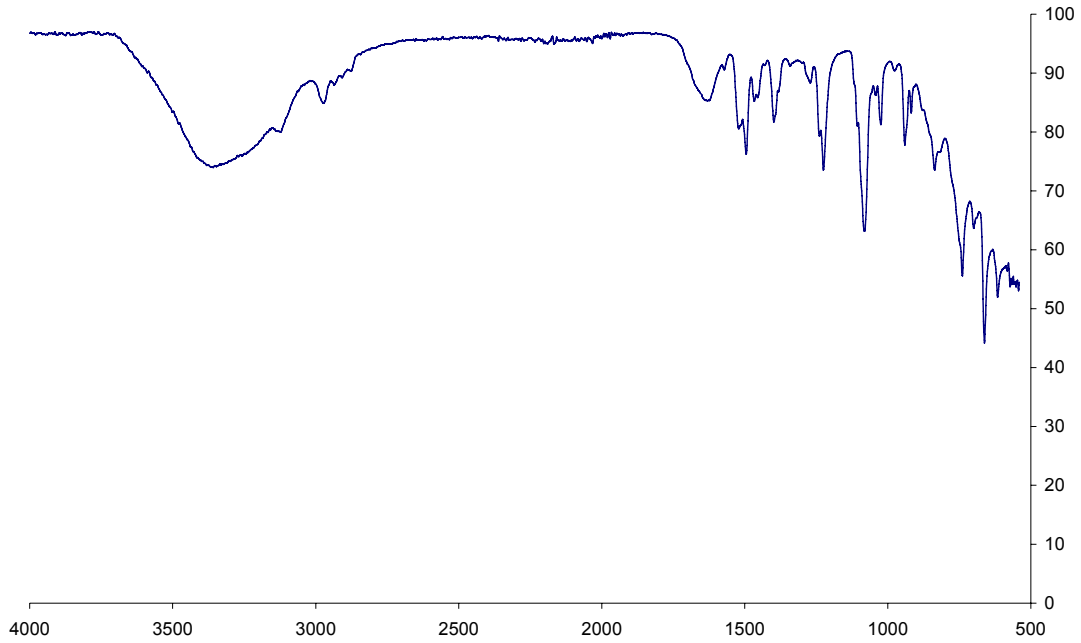

Figure S17: IR spectrum of TIF 2 after water vapour diffusion.

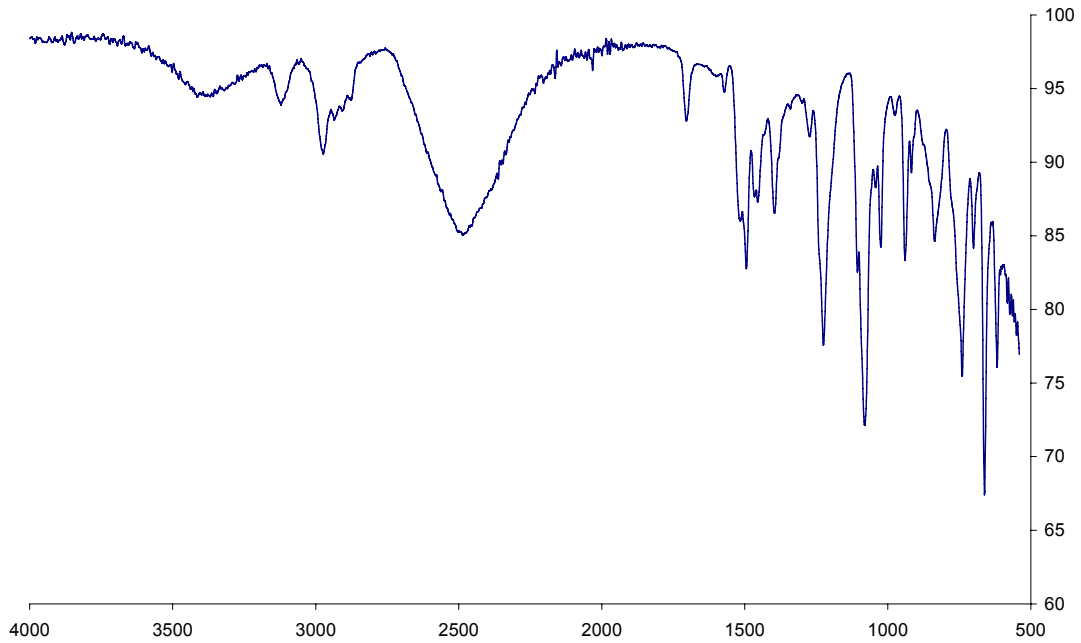

Figure S18: IR spectrum of TIF 2 after D_2O vapour diffusion.

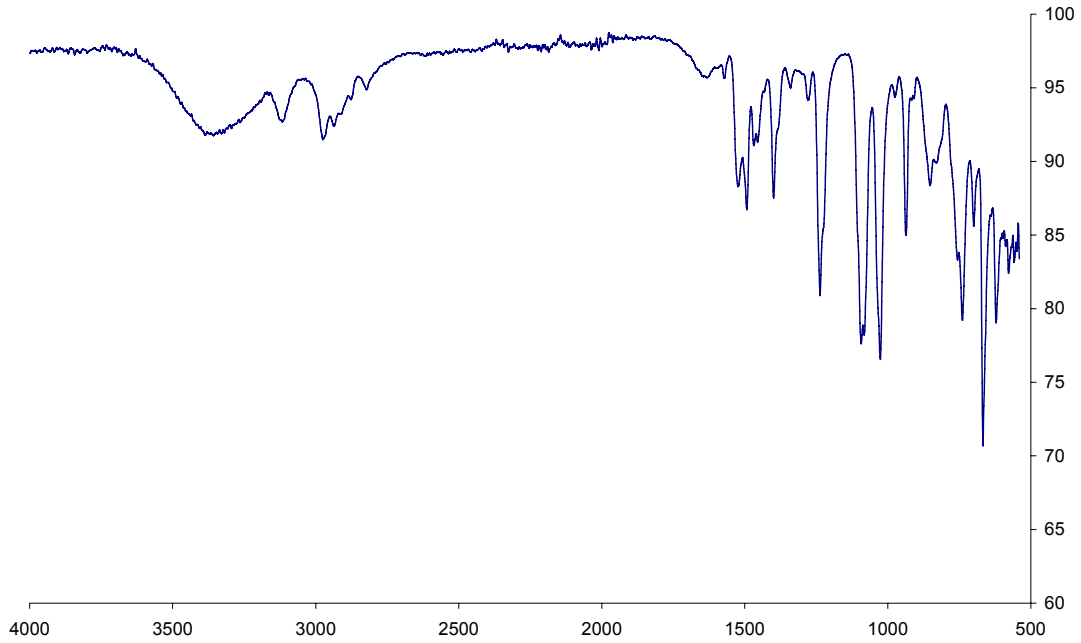

Figure S19: IR spectrum of TIF 2 after MeOH vapour diffusion.

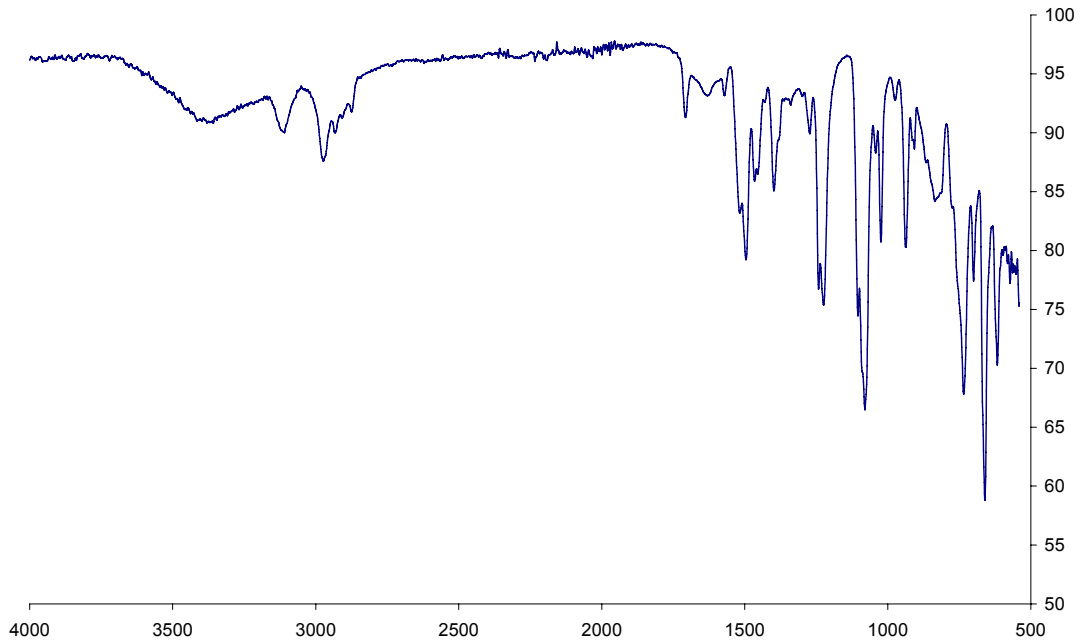

Figure S20: IR spectrum of TIF 2 after DCM vapour diffusion.

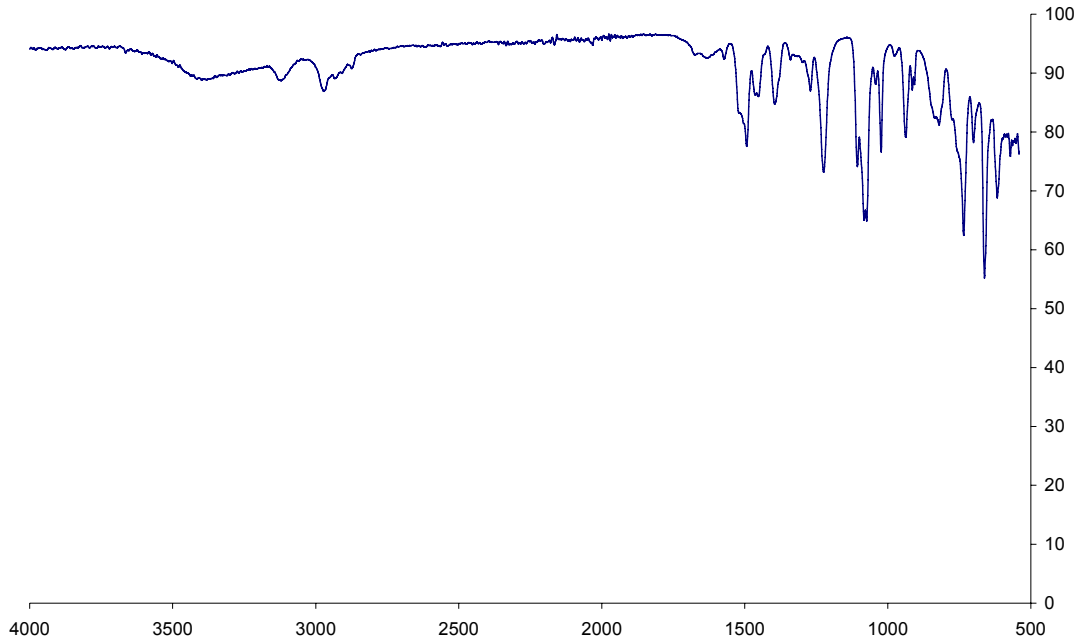

Figure S21: IR spectrum of TIF 2 after $CHCl_3$ vapour diffusion.

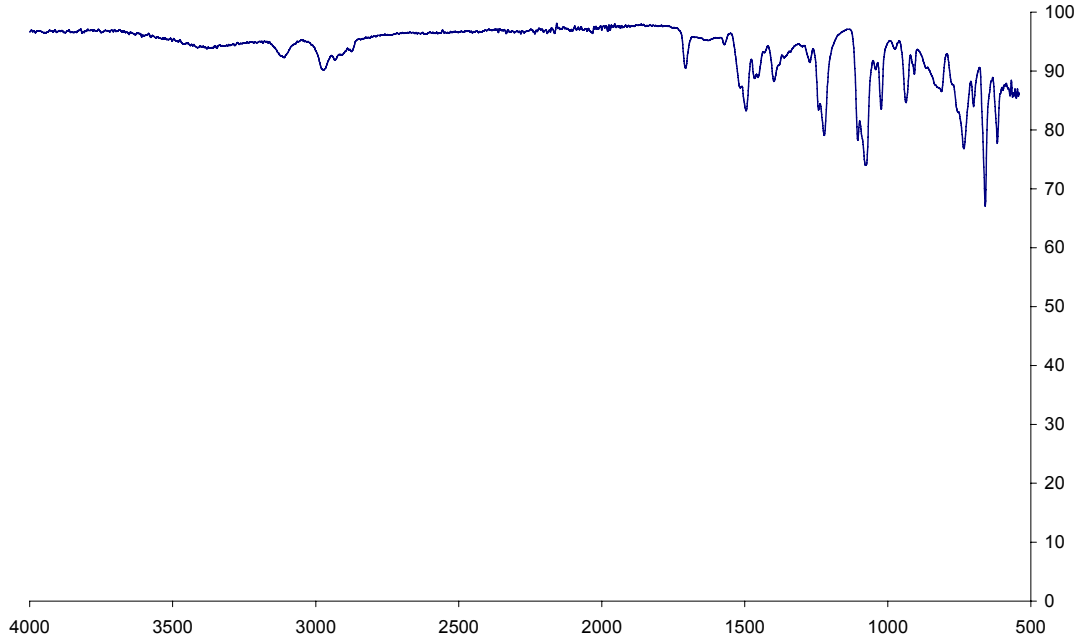

Figure S22: IR spectrum of TIF 2 after acetone vapour diffusion.

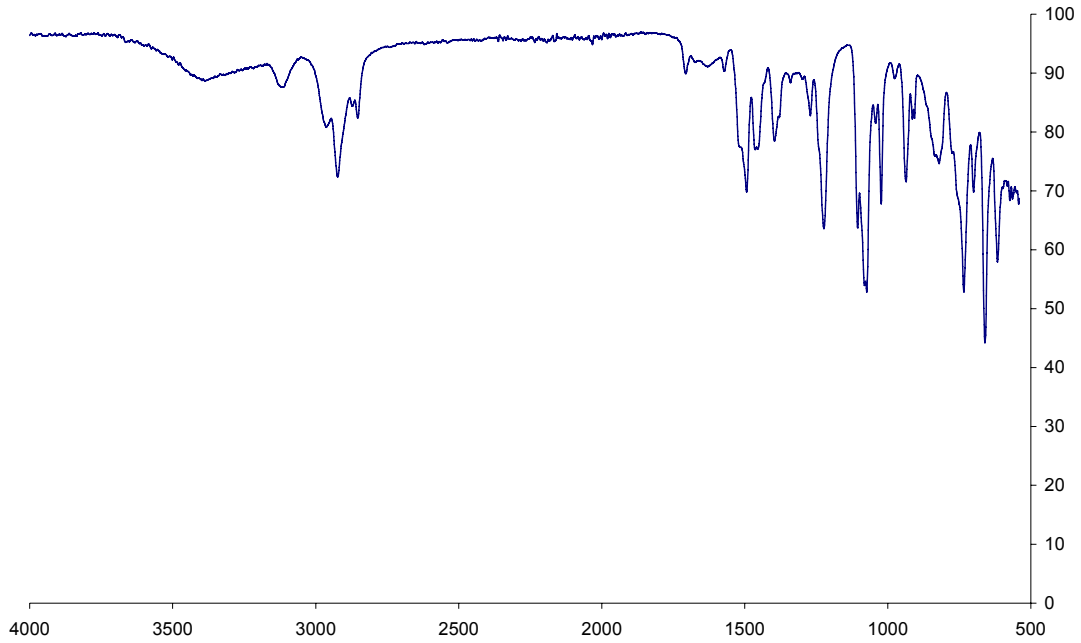

Figure S23: IR spectrum of TIF 2 after iodine vapour diffusion.

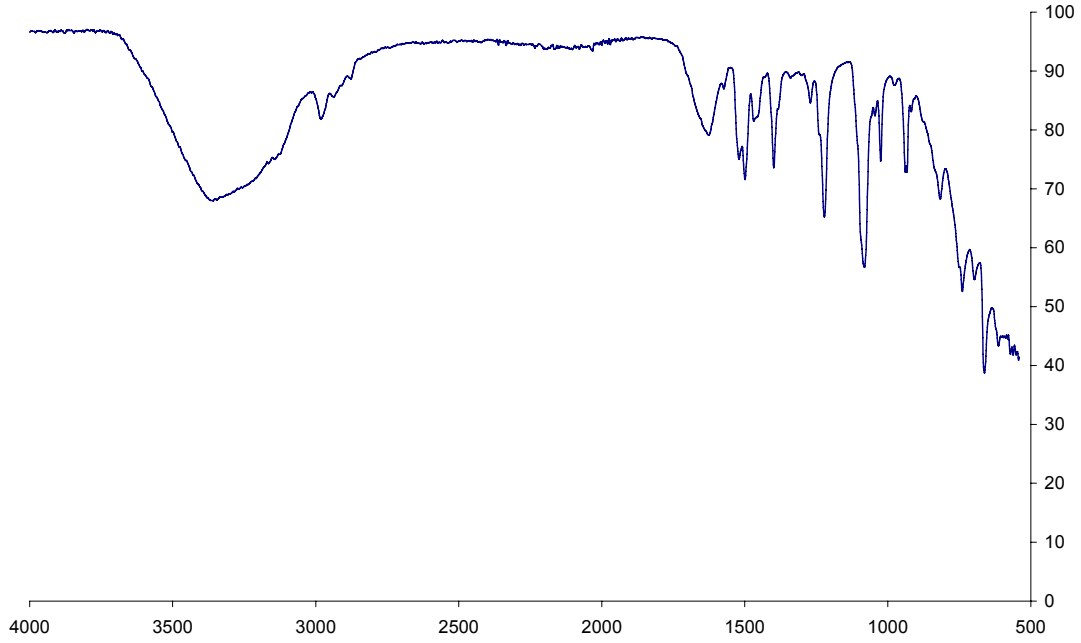

Figure S24: IR spectrum of TIF 3.

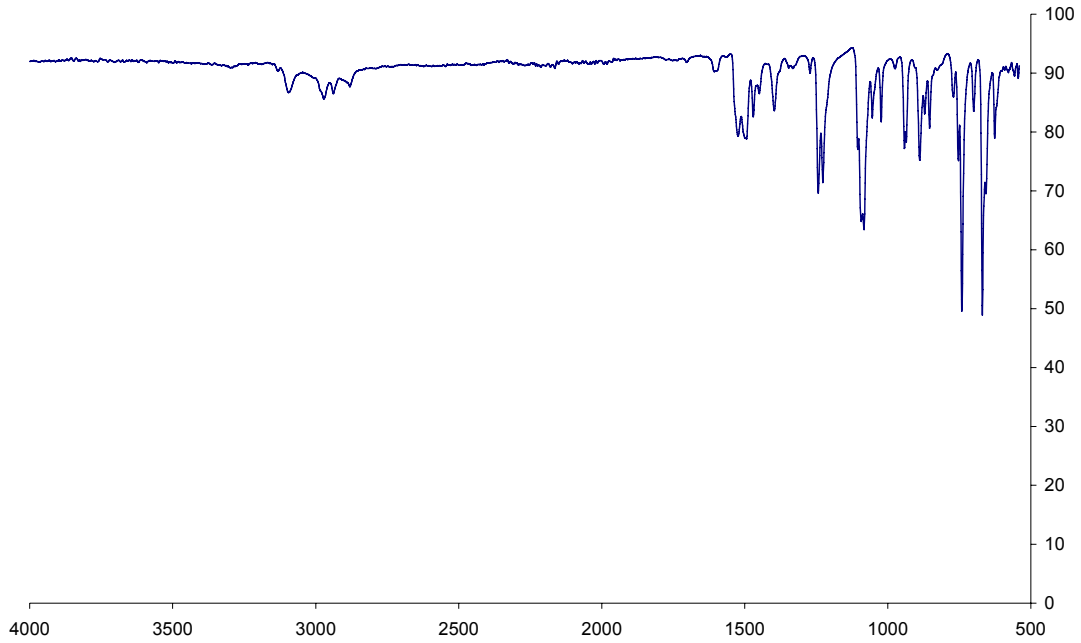

Figure S25: IR spectrum of TIF 3 after heating at 80 °C under vacuum.

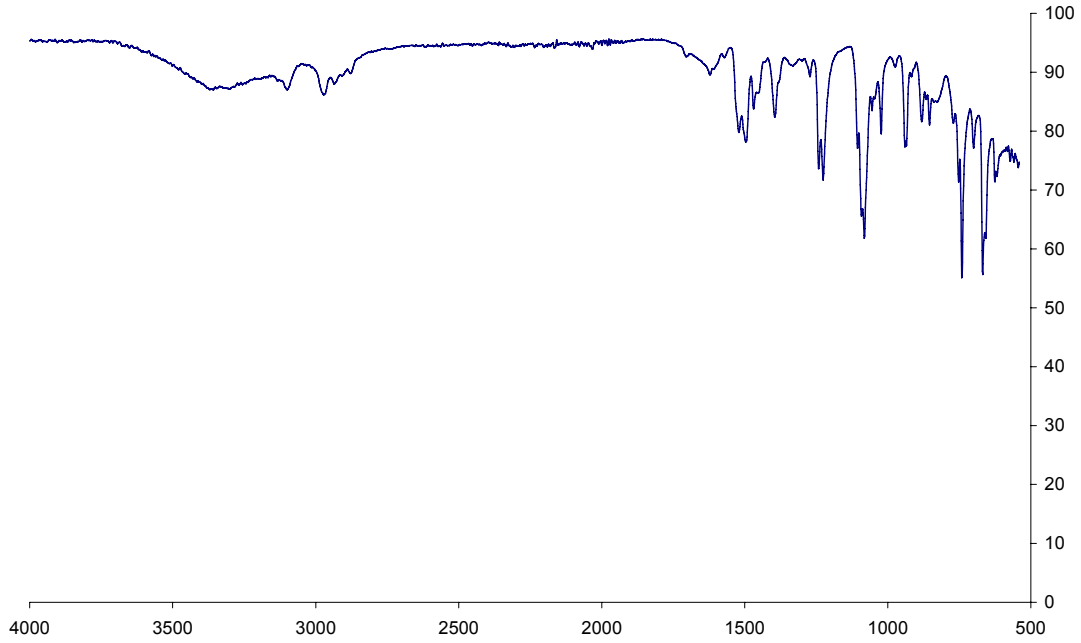

Figure S26: IR spectrum of TIF 3 after water vapour diffusion.

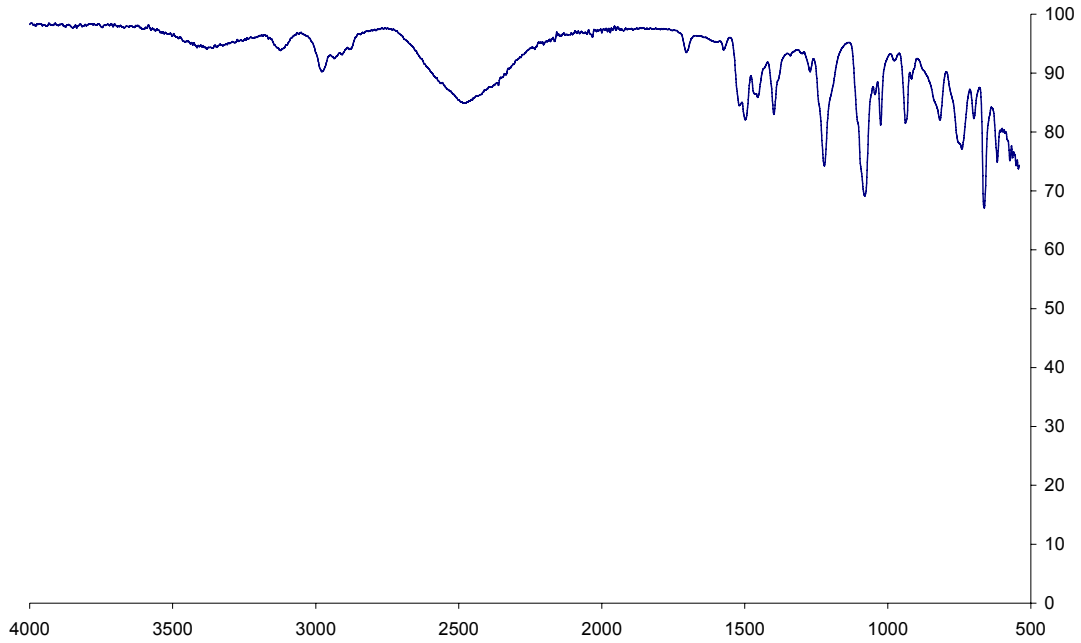

Figure S27: IR spectrum of TIF 2 after D_2O vapour diffusion.

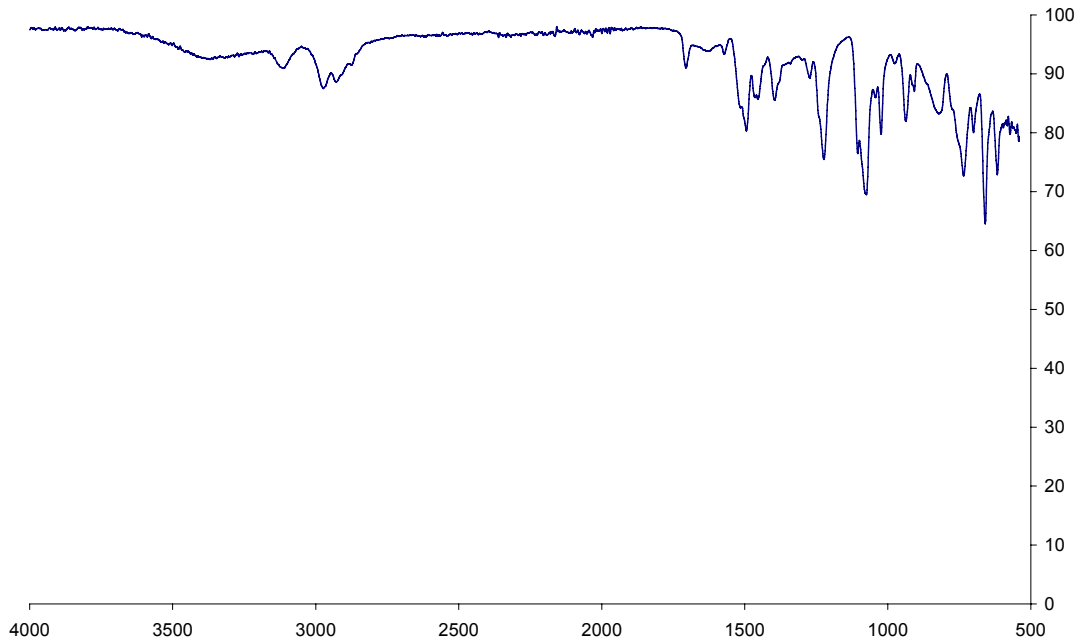

Figure S28: IR spectrum of TIF 2 after MeOH vapour diffusion.

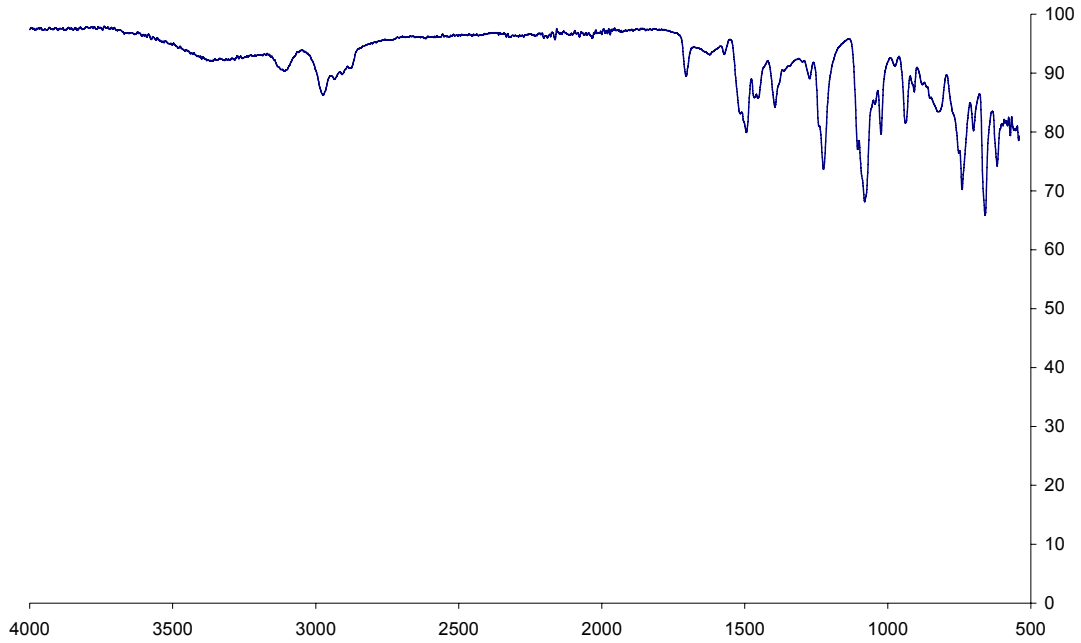

Figure S29: IR spectrum of TIF 2 after DCM vapour diffusion.

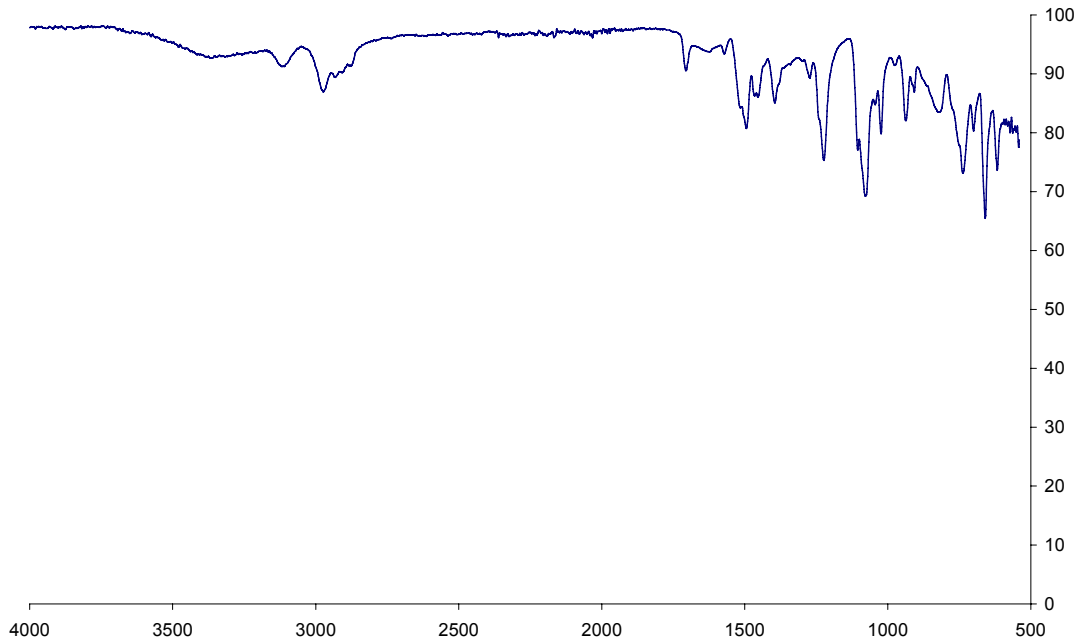

Figure S30: IR spectrum of TIF 2 after $CHCl_3$ vapour diffusion.

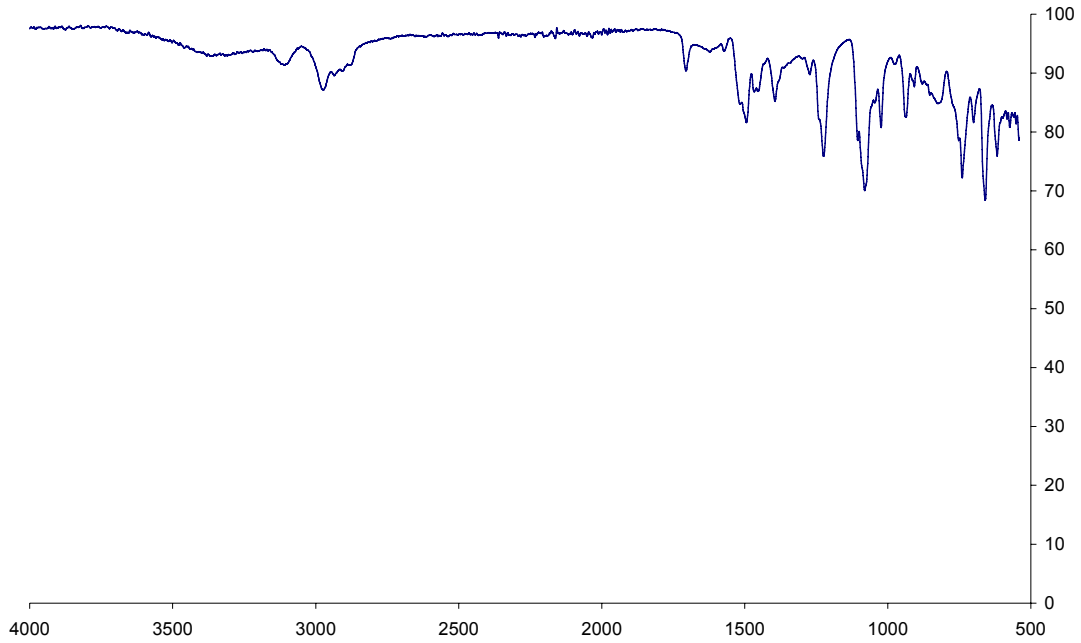

Figure S31: IR spectrum of TIF 2 after acetone vapour diffusion.

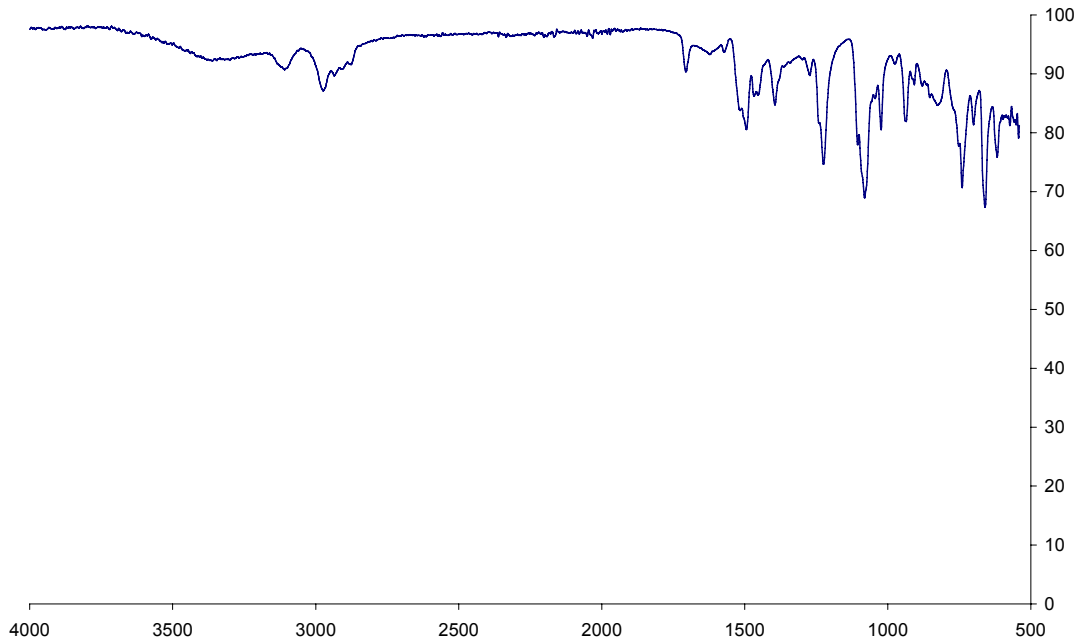

Figure S32: IR spectrum of TIF 2 after iodine vapour diffusion.